PII: S0032-3861(97)00379-0

Polymer Vol. 39 No. 5, pp. 1095–1102, 1998
© 1997 Elsevier Science Ltd
Printed in Great Britain. All rights reserved
0032-3861/97/$17.00+0.00

W.a.x.s. and force field constrained RIETVELD modelling of *meta*-linked fully aromatic copolyesters: 1. Poly(*p*-phenylene isophthalate)

Dieter Jehnichen[a,*], Peter Friedel[a], Jörg Bergmann[b], Thomas Taut[c], Josef Tobisch[a] and Doris Pospiech[a]
[a] *Institute of Polymer Research Dresden, Hohe Str. 6, D-01069 Dresden, Germany*
[b] *Ludwig-Renn-Allee 14, D-01217 Dresden, Germany*
[c] *Seifert-FPM GmbH Freiberg/Sa., Am St. Niclas Schacht 13, D-09599 Freiberg, Germany*
(Received 16 December 1996)

Fully aromatic copolyesters with regular chain structure containing kinked monomer units were investigated by powder diffraction experiments combined with structure modelling. Temperature dependent X-ray measurements show the existence of low and high temperature solid state modifications of poly(*p*-phenylene isophthalate), (IPA-HQ)$_n$. From the X-ray scattering data, *d*-spacings were determined taking some experimental corrections into account. Lattice parameters as well as atom coordinates of *lt*-(IPA-HQ)$_n$ were calculated and optimised by means of modelling procedures based on force field constrained RIETVELD algorithms. From this, a monoclinic unit cell of *lt*-(IPA-HQ)$_n$ with $a = 0.775$ nm, $b = 0.567$ nm, $c = 2.410$ nm, $\beta = 91.8°$ was found considering the chemical structure as well as interactions between the particles. The (IPA-HQ)$_n$ polyester is a typical representative of this kind of polymer with kinked monomeric, and hence is useful for further structural investigations. © 1997 Elsevier Science Ltd. All rights reserved.

(Keywords: kinked aromatic copolyesters; wide-angle X-ray scattering; molecular modelling)

INTRODUCTION

Aromatic liquid–crystalline main chain copolyesters with either random or regular chain structure are topics of many papers dealing with their rigid chain structure, their synthesis and processing conditions, leading to excellent mechanical and thermal characteristics (see for example Refs. [1–3]). Correlations between structure and processing parameters, first, and material properties, second, have been discussed widely. However, basic understanding of the influence of the chemical structure on parameters such as crystallinity and solid phase structure has to be further developed.

A previous paper[4] embarked on the process of clarifying whether model compounds, i.e. high crystalline aromatic copolyesters with defined regular chain structure, are useful in furthering current understanding of structure–property relationships. With respect to this goal, the polymers (TPA-HQ)$_n$ and (HBA-TPA-HBA-HQ)$_n$ (containing the monomer units terephthalic acid, TPA, hydroquinone, HQ, *p*-hydroxybenzoic acid, HBA) were investigated and found to have a monoclinic crystalline structure (space group P$\bar{1}$) with comparable unit cell parameters.

Following this, wide-angle X-ray scattering (w.a.x.s.) measurements combined with molecular modelling calculations were carried out on *meta*-linked regular aromatic copolyesters, starting with poly(*p*-phenylene isophthalate), (IPA-HQ)$_n$. Although the influence of kinked monomeric units has been discussed for some years, a basic understanding supported by detailed molecular modelling does not exist but seems to be necessary for the understanding of more complicated structures. (IPA-HQ)$_n$ shows two solid state modifications appearing at different temperatures. The existence ranges have to be determined for a correct interpretation of the X-ray diffractograms measured.

The *d*-spacings of *lt*-(IPA-HQ)$_n$ obtained from the X-ray scattering data were determined taking a few experimental corrections into account. Then, lattice parameters were calculated and optimised by means of modelling procedures based on force field constrained RIETVELD algorithms for the first time for copolyesters of such structure. Therefore, calculations using a monoclinic symmetry as suggested by other authors[5] and own experiences[4] were carried out.

A further aim of the investigation was to determine whether it is possible to obtain more information about the solid state structure of polymeric powders with a lower degree of ordering which usually cannot be investigated by single crystal measurements. This is a basic question in the field of polymer research.

EXPERIMENTAL

*Synthesis and characterisation of poly(*p*-phenylene isophthalate)*

Poly(*p*-phenylene isophthalate), (IPA-HQ)$_n$, was synthesised by reaction of isophthaloyl dichloride with hydroquinone in 1-chloronaphthaline at 240°C as described earlier[4].

Infra-red (i.r.) spectroscopy (on KBr): 1731 ($C{=}O_{ester,ar}$), 1508/1498 ($\nu C{-}C_{ar}$), 1173 ($\nu C{-}O{-}C_{ar}$), 1014, 721 ($\delta(C{-}H)_{ar}$) cm^{-1}.

---

[*] To whom correspondence should be addressed

Elemental analysis: C, 69.33% (calc. 70.00%); H, 3.17% (3.36%); O, 27.42% (26.64%).

Further chemical analysis could not be carried out because of the insolubility of $(IPA\text{-}HQ)_n$ in all solvents.

The melting temperature observed on a hot stage polarising microscope, as also found by temperature dependent w.a.x.s., is located near 380°C. The decomposition maximum found by differential thermal analysis is 523°C.

Wide angle x-ray diffraction

W.a.x.s. investigations were performed applying CuK_α radiation in a scattering range $2\Theta = 3\ldots50°$ with step width of $\Delta 2\Theta = 0.05°$ and counting time per step $\Delta t = 125$ s using the device system X-ray diffractometer HZG 4/A-2 (Seifert-FPM GmbH, Freiberg i. Sa., Germany) equipped with an energy-dispersive detector EDR 288 (RönTec GmbH, Berlin, Germany). The beam divergences were reduced by a primary vertical SOLLER collimator 0.5/25 and by horizontal slits allowing about 1.4°. The transmission technique was chosen to diminish preferred orientations of the sample.

Some temperature dependent measurements were carried out by using the w.a.x.s. devices of the polymer beamline A2 of HASYLAB facilities at DESY Hamburg (Germany) working with a linear detector and an oven up to 400°C.

Modelling

Modelling was carried out by means of IBM RISC SYSTEM 6000 with operating system AIX 3.2 (IBM Corp., 1993).

Monomer units. The geometry optimisation and conformation of monomer units was performed using the software GAMESS[6] for quantum mechanical ab initio calculations.

Polymer chains. Single polymer chains were built by the software package BUILDER[7], an interpreter connecting atomic models of residues in order to build blocks and then to polymerise these blocks to a chosen degree of polymerisation.

Crystal structure. Crystal packing and calculation of X-ray diagrams were executed by using the program package SYMMETRY (user interface and interpreter for modules CRYSTAL and XRAY[8]) in order to determine a qualified starting point for RIETVELD refinement.

Refinement. By means of software package BGMN[9] based on a modified RIETVELD algorithm similar to that described in the literature[10,11], a refinement of atomic coordinates using internal parameters within the unit cell was accomplished. Parameters depending on device and sample conditions can also be considered (see Appendix A).

Force field. The usual RIETVELD algorithm was expanded by a force field calculation of the crystalline structure with periodic boundary conditions. This was done to evaluate the structure during each step of approximation. In addition, the energy of the system was used as a further optimisation criterion, as well as the difference between calculated and experimental diffractograms (see Appendix A).

Graphic representations were executed by CERIUS^2 1.5[12], Xmol 1.3.1[13] and GNUPLOT 3.5[14].

X-RAY MEASUREMENTS

Wide angle X-ray diffraction measurements were carried out to continue the structure investigations of high aromatic copolyesters[4] containing kinked monomer units. For direct comparison of $(IPA\text{-}HQ)_n$ with polymers prepared earlier, the sample was synthesised and prepared in the same manner.

Wide angle X-ray diffractograms of the two solid state structures corresponding to the low (*lt*) and high (*ht*) temperature modification are shown in *Figure 1*. The transition temperature $T_{lt \rightarrow ht}$ is about 260°C, T_m is found near 380°C (cf. *Figure 2*). *lt*-$(IPA\text{-}HQ)_n$ was synthesised by low temperature solution polycondensation conditions reported earlier[4] (or by a similar procedure[15]), whereas the *ht*-modification originates from melt polycondensation[16] or can be obtained by annealing within the temperature range of existence of this structure as well as by slow cooling from the melt.

Owing to similarities in the molecular architecture of the family of fully aromatic main chain copolyesters, it was supposed that the polymer under discussion is also characterised by a monoclinic symmetry which would be helpful for the formal indication of the reflections. However, the chemical individuality of $(IPA\text{-}HQ)_n$ has to manifest itself in differences in the reflection intensities. To support the formal results, calculations were carried out using methods of molecular modelling. Since the measuring data are not complete enough to obtain the crystal structure directly, it seemed reasonable to get more structural information by modelling.

CALCULATION METHODS

The crystal structure was calculated from the experimental data by the following fitting procedures.

Monomers and polymer chain

The procedure used to build the polymer chain was described earlier[4]. From ab initio calculations (basis set STO-6G) of the monomer units (IPA, HQ) and a dimeric model unit (phenylene benzoate) it was concluded that the phenyl rings can be regarded as planar. The ester moiety lies approximately in the same plane as the outer phenylene ring of the complex aromatic unit, whereas the phenylene ring following the diol unit turns out of the plane because of steric hindrances combined with *para*-interactions of the phenyl rings over the ester unit (see also Refs. [5,17,18]).

Looking for conformations of the polymer chains which are energetically preferred and most extended, the *cis*-conformation of IPA (also favoured by Johnson *et al.*[19–21]) was chosen to connect the monomer units. Consequently, a kink in the polymer chain is created. Two kinks with opposite direction per crystallographic repeating unit, consisting of two IPA-HQ sequences (see also *Figures 3* and *4*), are necessary to obtain an extended polymer chain.

Calculation of the unit cell parameters

Parameters of monoclinic symmetry similar to those of a previous work[4] were used to analyse the basic scattering data, applying the program BGMN which performs an approximation with direct convolution based peak profiles. It should be noted that this calculation step does not include the consideration of any internal structure of the crystallographic cell. With respect to a measured instrumental function *versus* scattering angle which determines the peak

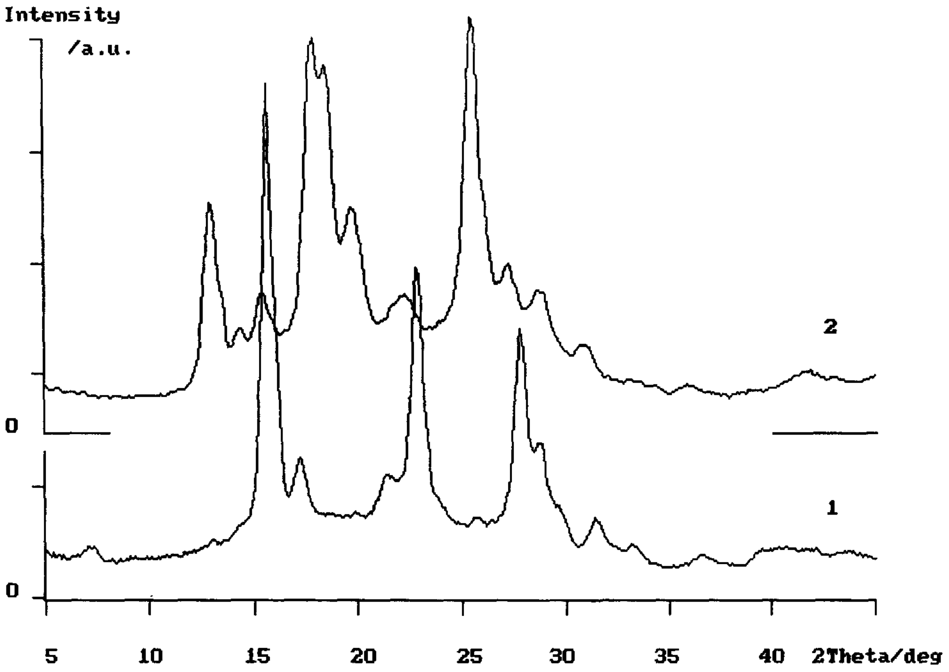

Figure 1 W.a.x.s. curves of the low (1, *lt*) and high (2, *ht*) temperature modification of $(IPA\text{-}HQ)_n$, measured at room temperature

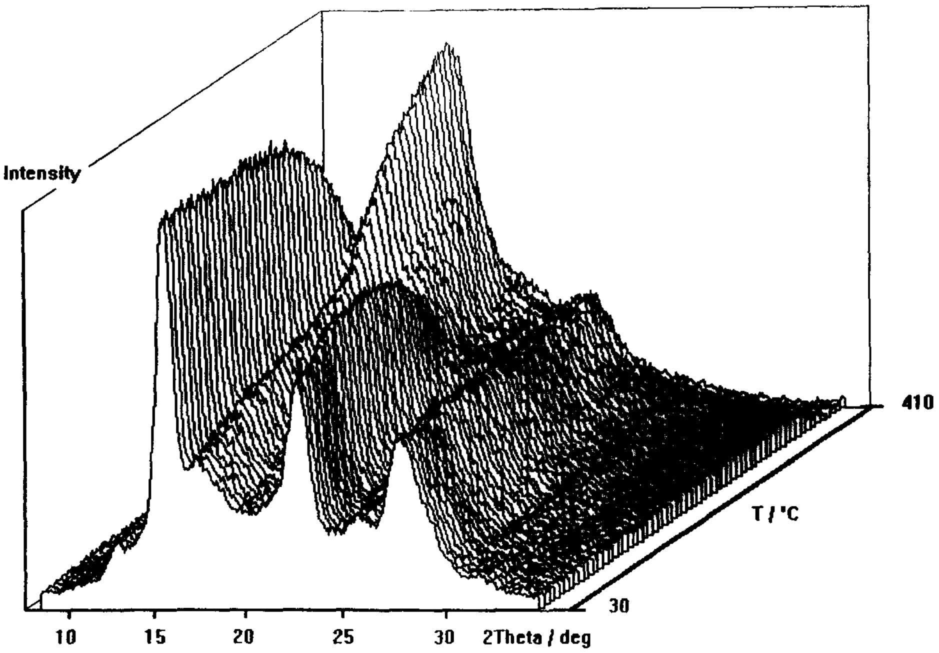

Figure 2 Temperature dependent w.a.x.s. diagram of $(IPA\text{-}HQ)_n$

profile, the computed reflections were approximated to the experimental scattering data containing their position, height, and full width at half maximum. The structure factor F was not calculated during this step. The approximation was evaluated by minimisation of the performance coefficient Q_{RIETVELD} providing the R-parameter with

$$R^2_{\mathrm{RIETVELD}} = \frac{Q_{\mathrm{RIETVELD}}}{\sum_{2\Theta} w_{2\Theta} \cdot I^2_{\mathrm{exp}}(2\Theta)} = \frac{\sum_{2\Theta} w_{2\Theta} \cdot (I_{\mathrm{exp}}(2\Theta) - I_{\mathrm{calc}}(2\Theta))^2}{\sum_{2\Theta} w_{2\Theta} \cdot I^2_{\mathrm{exp}}(2)} \qquad (1)$$

$w_{2\Theta}$-weighting factor according to counting statistics

The lattice parameters calculated structure-less (a = 0.840 nm, b = 0.566 nm, c = 2.464 nm, β = 96.0°) serve as starting values for the search for symmetry and the crystal packing. The corresponding R-parameter amounts to 2.6%.

Search for symmetry

The X-ray data were tested for reflection conditions with respect to the monoclinic symmetry. These calculations result in the space group Pc (No. 7 of International Tables[22]) with glide plane **n**.

Crystal packing

First, a single crystallographic repeating unit of the polymer chain is packed so that the centre of mass lies at the coordinate origin, and the chain is oriented along the main axes of its inertia moments with its greatest value along the z-axis and the smallest along the x-axis. Second, some twist

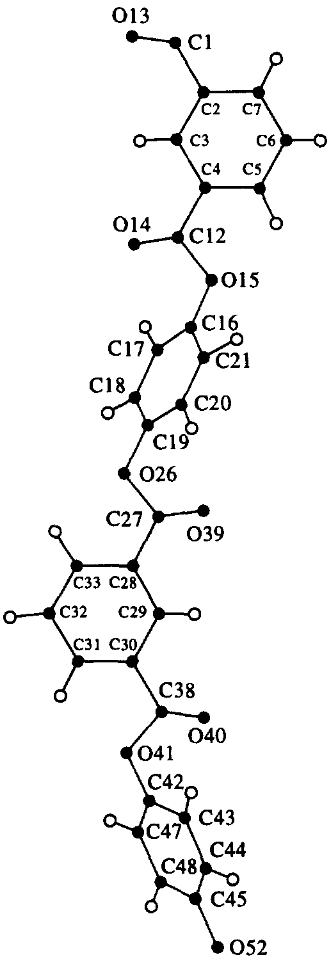

Figure 3 Schematic view on the polymer chain of (IPA-HQ)$_n$ including force field atom types

angles ρ_3, ρ_2, ρ_1 (regarding rotations around the cartesian *z*-, *y*- and *x*-axes, respectively) and also a shift vector **SP**(*xx*,*yy*,*zz*) were scanned. This was necessary in order to obtain a good estimation of the chain orientation as a starting point for the RIETVELD refinement.

Force field constrained structure refinement

The force field constrained RIETVELD structure refinement is a combined minimisation of both the conventional RIETVELD part Q_{RIETVELD} (equation (1)) which is determined by the structure factor and a force field part Q_{FF} (equation (3), see below), expressing the energetical relevance of the approximated structure. The coupling was carried out by means of an extended *Q*-parameter as follows

$$Q^*_{\mathrm{RIETVELD}} = c_{\mathrm{Theory}} \cdot Q_{\mathrm{FF}} + Q_{\mathrm{RIETVELD}} \qquad (2)$$

where the calibration coefficient c_{Theory} is usually chosen as 1 mol kcal^{-1}. Both criteria are sufficient to characterise the refined structure.

RIETVELD. The twist angles ρ_1, ρ_2, ρ_3 (see *Table 1*) and also the shift vector **SP**(0,*yy*,0) were chosen as parameters for motion of the whole molecule. Additionally, bonding and torsion angles (see *Table 2*) are used as internal parameters because of their great influence on scattering behaviour. The bonding distances may not have such an effect.

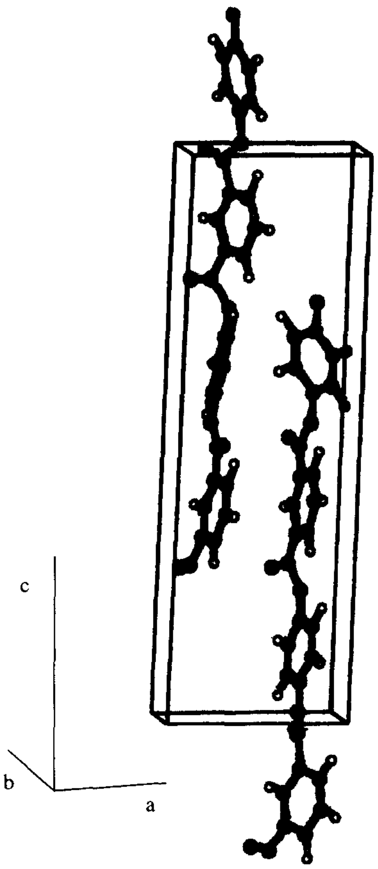

Figure 4 Perspective view into the monoclinic cell of *lt*-(IPA-HQ)$_n$

Table 1 Calculated lattice and orientation parameters of *lt*-(IPA-HQ)$_n$

Monoclinic lattice	*a* (nm)	0.775 ± 0.001
Space group:	*b* (nm)	0.567 ± 0.001
Pc (No. 7)	*c* (nm)	2.410 ± 0.006
	β (deg)	91.8 ± 0.2
	V (nm^3)	1.06 ± 0.01
	Z	2
	ρ_x (g cm^{-3})	1.50 ± 0.01
Twist angles	ρ_3 (deg) (*z*-axis)	− 31.7 ± 2.9
	ρ_2 (deg) (*y*-axis)	10.8 ± 1.7
	ρ_1 (deg) (*x*-axis)	10.6 ± 2.1
Shift vector **SP**	*xx* (nm)	–[a]
	yy (nm)	0.01 ± 0.03
	zz (nm)	–[a]

[a] No conditions because of the glide planes

Force field. The force field part is given by the sum term

$$Q_{\mathrm{FF}} = Q_{\mathrm{bd}} + Q_{\mathrm{nbd}} \qquad (3)$$

There are bonding and nonbonding interactions defining a force field, as has often been described[23,24]. For the calculations reported here, only nonbonding interactions of a general Van der Waals type model given by

$$Q_{\mathrm{nbd}} = \sum_{i,j} (A_{ij} \cdot r_{ij}^{-12} + B_{ij} \cdot r_{ij}^{-6}) \text{ with } i < j \qquad (4)$$

$$\text{using } A_{ij} = \varepsilon_{ij,\mathrm{eq}} \cdot r_{ij,\mathrm{eq}}^{12} \text{ and } B_{ij} = -2 \cdot \varepsilon_{ij,\mathrm{eq}} \cdot r_{ij,\mathrm{eq}}^{6}$$

$$\varepsilon_{ij,\mathrm{eq}} = \sqrt{\varepsilon_i \cdot \varepsilon_j} \text{ and } r_{ij,\mathrm{eq}} = (r_i + r_j)$$

and bonding interactions in the form of so-called penalty functions with respect to harmonic oscillator potentials like

$$Q_{\mathrm{bd}} = \sum_b f_b \cdot (r_b - r_{b,\mathrm{eq}})^2 + \sum_v f_v \cdot (\delta_v - \delta_{v,\mathrm{eq}})^2 \qquad (5)$$

were used. The nonbonding interactions have been applied to all atoms (*Figure 3*), which means that all atoms interact with each other within a determined cutting radius of $3r_{ij,\mathrm{eq}}$. The parameters used for various atom types (see *Table 3*) are given in *Table 4*.

The parameters of bonding interactions are given in *Table 5*. Note that the oscillation constants used are excessive in relation to i.r. spectroscopic ones because of the chain continuation required. In the process only the following penalty functions were used.

Table 2 Refined bonding angles A_x–A_y–A_z and torsion angles B_w–B_x–B_y–B_z in comparison with the corresponding values from ab initio calculations

Kind of angle	Angle$_{\mathrm{RIETVELD}}$ (deg)	Angle$_{\mathrm{ab\ initio}}$ (deg)
C4–C12–O15	117.0	111.5
C12–O15–C16	110.4	115.1
C19–O26–C27	120.4	115.1
O26–C27–C28	112.3	111.5
C30–C38–O41	101.5	111.5
C38–O41–C42	110.8	115.1
C45–O52–C1$_n^a$	115.0	115.1
O52–C1$_n$–C2$_n^a$	92.2	111.5
C5–C4–C12–O15	35.9	0.3
C4–C12–O15–C16	175.1	177.0
C12–O15–C16–C17	25.0	55.6
C18–C19–O26–C27	127.9	124.4
C19–O26–C27–C28	167.3	177.0
O26–C27–C28–C29	162.3	175.8
C31–C30–C38–O41	4.8	0.3
C30–C38–O41–C42	176.3	177.0
C38–O41–C42–C43	63.9	55.6
C44–C45–O52–C1$_n^a$	163.0	124.4
C45–O52–C1$_n$–C2$_n^a$	173.5	177.0
O52–C1$_n$–C2$_n$–C3$_n^a$	150.0	175.8

[a] Index n means the named atom in the next unit cell in *z*-direction

RESULTS AND DISCUSSION

Up to $2\Theta = 35°$, 64 reflections were found as significant because of the calculated unit cell parameters. With the result of the structure-less approximation, all possible combinations of symmetry operators were tested. The space group Pc with mirror glide plane **n** and unique axis *b* supplies the best approximation of structure parameters including energy minimisation with $R_{\mathrm{RIETVELD}} = 7.4\%$. The corresponding minimal *Q*-parameters amount to $Q_{\mathrm{nbd}} = -5556\ \mathrm{kcal\ mol^{-1}}$ and $Q_{\mathrm{bd}} = 5898\ \mathrm{kcal\ mol^{-1}}$, respectively.

The unit cell parameters obtained by refinement are given in *Table 1*. The comparison of experimental and calculated powder diagrams is shown in *Figure 5*. *Table 6* contains the reflections including their structure factors and relative intensities with $L_{\mathrm{rel,calc}} \geq 1\%$. *Table 3* gives the fractional atom coordinates.

The values of refined bonding and torsion angles (*Table 2*) valid for the crystal are significantly changed with respect to the ab initio ones of the free molecule. This results in a 'bended' structure of the polymer chain with respect to their intermolecular interactions inside the crystal. *Figure 4* shows the monoclinic unit cell including two polymer chains with respect to the symmetry conditions found. Isophthalic acid units seem to be nearly planar, whereas hydroquinone units alternate between planar and perpendicular orientations. One can imagine both isophthalic acid and hydroquinone units arranged into 'layers' parallel to the *ab*-plane. It should be noted that the neighbouring ones in the *a*-direction have a reverse conformation.

FUTURE PROSPECTS

The goal of this work was the clarification of solid state structure of *meta*-linked regular aromatic copolyesters, i.e. $(\mathrm{IPA\text{-}HQ})_n$, by means of a skilful combination of powder diffraction experiments with molecular modelling procedures. Force field constrained RIETVELD algorithms were used successfully for the first time in this field of investigation.

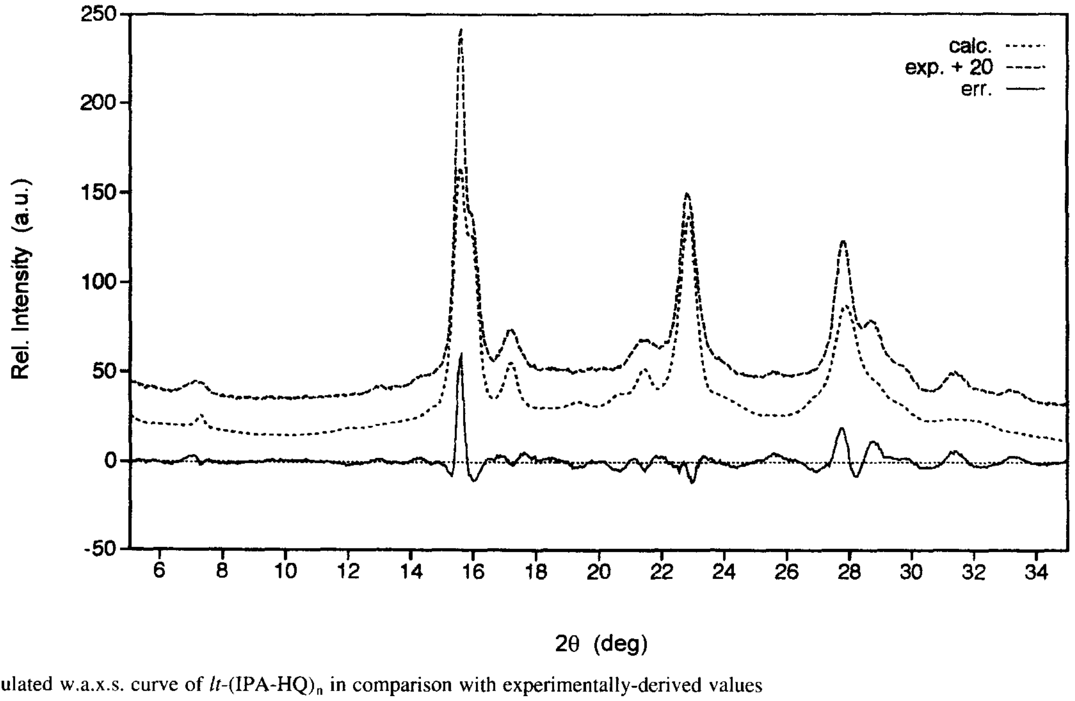

Figure 5 Calculated w.a.x.s. curve of *lt*-$(\mathrm{IPA\text{-}HQ})_n$ in comparison with experimentally-derived values

Table 3 Fractional atom coordinates of *lt*-(IPA-HQ)$_n$

Atom	Residuum	*x*	*y*	*z*
C1	IPA	− 0.125	− 0.029	− 0.473
C2	IPA	− 0.203	− 0.166	− 0.426
C3	IPA	− 0.191	− 0.078	− 0.371
C4	IPA	− 0.264	− 0.204	− 0.328
C5	IPA	− 0.348	− 0.419	− 0.339
C6	IPA	− 0.360	− 0.507	− 0.393
C7	IPA	− 0.287	− 0.381	− 0.436
H8	IPA	− 0.126	0.089	− 0.363
H9	IPA	− 0.404	− 0.517	− 0.305
H10	IPA	− 0.425	− 0.674	− 0.401
H11	IPA	− 0.297	− 0.449	− 0.479
C12	IPA	− 0.253	− 0.114	− 0.268
O13	IPA	− 0.049	0.157	− 0.471
O14	IPA	− 0.263	0.095	− 0.259
O15	HQ	− 0.232	− 0.283	− 0.226
C16	HQ	− 0.239	− 0.175	− 0.174
C17	HQ	− 0.196	0.063	− 0.168
C18	HQ	− 0.203	0.170	− 0.116
C19	HQ	− 0.253	0.039	− 0.070
C20	HQ	− 0.295	− 0.200	− 0.076
C21	HQ	− 0.289	− 0.307	− 0.128
H22	HQ	− 0.158	0.165	− 0.204
H23	HQ	− 0.170	0.356	− 0.111
H24	HQ	− 0.334	− 0.302	− 0.040
H25	HQ	− 0.322	− 0.493	− 0.133
O26	HQ	− 0.258	0.153	− 0.018
C27	IPA	− 0.171	0.058	0.028
C28	IPA	− 0.224	0.176	0.082
C29	IPA	− 0.189	0.065	0.133
C30	IPA	− 0.237	0.173	0.182
C31	IPA	− 0.320	0.392	0.181
C32	IPA	− 0.355	0.503	0.130
C33	IPA	− 0.307	0.395	0.080
H34	IPA	− 0.124	− 0.106	0.134
H35	IPA	− 0.358	0.476	0.219
H36	IPA	− 0.419	0.674	0.129
H37	IPA	− 0.333	0.481	0.041
C38	IPA	− 0.202	0.058	0.239
O39	IPA	− 0.067	− 0.100	0.025
O40	IPA	− 0.127	− 0.118	0.255
O41	HQ	− 0.283	0.215	0.274
C42	HQ	− 0.275	0.132	0.329
C43	HQ	− 0.357	− 0.079	0.343
C44	HQ	− 0.349	− 0.162	0.397
C45	HQ	− 0.257	− 0.034	0.438
C46	HQ	− 0.175	0.177	0.425
C47	HQ	− 0.183	0.259	0.370
H48	HQ	− 0.428	− 0.178	0.311
H49	HQ	− 0.413	− 0.326	0.408
H50	HQ	− 0.103	0.276	0.457
H51	HQ	− 0.119	0.423	0.359
O52	HQ	− 0.252	− 0.124	0.492

Based on general structural principles which can be assumed on the basis of similar chain structure, a good agreement of experimental and calculated data was found. Moreover, in addition to the unit cell parameters a complete set of atomic coordinates was computed with high probability if additional conditions with respect to the chemical structure and interactions were considered. Hence, it should be possible to correlate the primary chemical structure and some molecular characteristics with crystallographic data as well as to understand some aspects of the phase behaviour and a few material properties.

The results obtained encourage the continuation of such combined investigations of w.a.x.s. and molecular modelling with other crystalline copolyesters.

Table 4 Parameters of atom types used in nonbonding interactions

Atom type	r_i (nm)	ϵ_i (kcal mol^{-1})
C	0.185	0.12
H	0.154	0.10
OS (C=O)	0.165	0.15
OE (C–O)	0.160	0.20

r_i, Van der Waals radii; ε_i, potential wall depths

ACKNOWLEDGEMENTS

The Deutsche Forschungsgemeinschaft is gratefully acknowledged for financial support of this work.

APPENDIX A:

Structure modelling of crystalline polymers based on X-ray

Table 5 Parameters of penalty functions for bonding interactions

Atomic identifier	f_b resp. f_v	$r_{b,\mathrm{eq}}$ resp. $\delta_{v,\mathrm{eq}}$
052–C1$_n^a$	1.44×10^6 kcal mol^{-1} nm^{-2}	0.132 nm
C45–052–C1$_n^a$	1.44×10^4 kcal mol^{-1} deg^{-2}	115°

f_b, f_v, oscillation constants; $r_{b,\mathrm{eq}}$, $\delta_{v,\mathrm{eq}}$, equilibrium values

[a] Index n means the named atom in the next unit cell in *z*-direction

Table 6 Comparison of experimental and calculated data ($I_{\mathrm{rel,calc}} \geq 1\%$)

I_{exp} (a.u.)	d_{exp} (nm)	d_{calc} (nm)	*h k l*	*H*	$\lvert F_{\mathrm{calc}} \rvert$	$I_{\mathrm{rel,calc}}$ (%)
m	1.218	1.2044	0 0 2	2	12.2	2.8
w	0.619	0.6022	0 0 4	2	19.8	1.8
vs	0.568	0.5672	0 1 0	2	139.3	80.1
		0.5665	− 1 0 3	2	22.4	2.1
s	0.550	0.5521	0 1 1	4	83.1	53.9
		0.5493	1 0 3	2	25.9	2.6
m	0.515	0.5131	0 1 2	4	52.8	18.7
		0.4577	1 1 0	4	21.8	2.5
		0.4305	− 1 1 2	4	29.3	4.0
		0.4253	1 1 2	4	25.8	3.0
m	0.414	0.4129	0 1 4	4	65.0	18.0
		0.4015	0 0 6	2	23.3	1.1
		0.4008	− 1 1 3	4	20.6	1.7
		0.3946	1 1 3	4	25.8	2.6
vs	0.389	0.3875	2 0 0	2	231.9	100.0
		0.3723	2 0 − 2	2	55.9	5.3
		0.3676	− 1 1 4	4	23.3	1.8
		0.3656	2 0 2	2	26.6	1.2
		0.3612	1 1 4	4	28.4	2.6
		0.3306	− 2 0 4	2	67.6	6.0
		0.3289	1 1 5	4	27.5	2.0
		0.3214	2 0 4	2	46.7	2.7
s	0.321	0.3200	2 1 0	4	114.9	32.4
		0.3183	2 1 − 1	4	99.5	23.9
		0.3161	2 1 1	4	82.3	16.2
m	0.310	0.3112	− 2 1 2	4	63.5	9.3
		0.3073	2 1 2	4	77.3	13.4
		0.3011	0 0 8	2	45.7	2.2
w	0.300	0.2999	− 2 1 3	4	53.2	6.0
m	0.285	0.2856	− 2 1 4	4	37.8	2.7
		0.2816	0 2 1	4	31.6	1.8
		0.2796	2 1 4	4	29.1	1.5
w	0.270	0.2760	0 2 2	4	48.9	4.2
		0.2577	3 0 − 1	2	44.9	1.5

powder data is a very complicated matter because of the limited number of observed peaks in the diffraction diagram. Sophisticated algorithms must be used to obtain the maximum information. The lack of a sufficient number of well-resolved peaks made conventional peak fitting and indexing impossible. The only way to get first information about the lattice was a lattice-constrained fit of the full diagram. Starting values for the lattice parameters were based on a proposal from molecular calculations.

Programs allowing such a lattice-constrained fit are often RIETVELD-like. They require a set of lattice parameters and, because of the absence of structural information, they fit each resulting reflection intensity individually. To reach a good fit suitable peak profiles have to be used. Simple analytical functions with angle-dependent peak widths ('u–v–w' formulae) are too inaccurate, particularly for scattering angles $2\Theta < 10°$.

To avoid problems regarding erroneous peak fits the program BGMN in its structure-less mode was used. This program contains an exact device adapted model of peak profiles. Thus, it is possible to use broad beam divergences in favour of a good measuring statistic since the program is able to handle extremely asymmetrical peaks at very small angles. As a contribution to peak broadening, up to three phase-related real-structure parameters can be refined. Multiple device geometries, especially the non-focusing transmission geometry of the presented scattering experiment are available. Also in this case an exact peak profile (box-like or trapeze-like) is calculated. Note that only the lattice parameters, the angle zero point, three real-structure parameters and all individual intensities were free in the calculation procedure.

In the next step a structural proposal again determined from molecular calculations is the starting point for an exact RIETVELD calculation. Normally all atom positions have to be entered in the RIETVELD input. This leads to a very large parameter number (the unit cell of *lt*-$(\text{IPA-HQ})_n$ contains 52 atoms in the general position). Because of the given molecular structure and the poor experimental data these parameters are not refinable independently. A suitable reduction of the parameter number is achieved by introduction of molecules instead of atoms in the calculation. A small number of RIETVELD programs are capable of handling molecules as rigid bodies (for example GSAS[25]).

The program BGMN introduces molecules not only as rigid bodies, but which can be shifted and rotated. Also torsions of molecular parts, changes of bond angles and bond lengths are built-in operations. Moreover, BGMN contains a mathematical formula interpreter which permits user-defined functions based on a special 'structure describing language'. Additionally, all parameters can be limited to avoid pointless conformations. By means of the formula interpreter geometric constraints were introduced. The goal of these constraints is the calculation of the crystalline structure with periodic boundary conditions. This ensures the appropriate continuation of the molecules from one unit cell to the next.

Nevertheless, for complex molecules it could be happen that misinterpreted minima of resulting fit functions are generated. Therefore, the number of free parameters must remain limited because of the small number of observed reflections. To overcome this parameter number restriction a unique feature was introduced by BGMN in the RIETVELD refinement: force field constraints. Such constraints are a serious precondition to avoid atom overlaps in the structure (a small number of interaction terms generates thousands of force field constraints in dependence of the actual crystal structure).

Only the geometric and force field restrictions allowed the calculation of a sufficient number of free conformation parameters with merely a small risk to find false minima of approximation procedures.

REFERENCES

1. Jackson, W. J. jr, *Molecular Crystals and Liquid Crystals*, 1989, **169**, 23–49.
2. Calundann, G. W., in *High Performance Polymers: Their Origin and Development*, ed. R. B. Seymour and G. S. Kirshenbaum. Elsevier, 1986, pp. 235–249.
3. Brewins, R. W., Daly, R. C. and Turner, S. R., in *Encyclopaedia of Polymer Science Engineering*, Vol. 9. John Wiley & Sons, New York/Chichester, 1987, pp. 1–61.
4. Jehnichen, D., Tobisch, J., Pospiech, D. and Friedel, P., *Polymer*, 1996, **37**, 1463–1475.
5. Coulter, P. D., Hanna, S. and Windle, A. H., *Liquid Crystals*, 1989, **5**, 1603–1618.
6. Schmidt, M. W., Baldridge, K. K., Boatz, J. A., Jensen, J. H., Koseki, S., Gordon, M. S., Nguyen, K. A., Windus, T. L. and Elbert, S. T., *QCPE Bulletin*, 1990, **10**, 52.
7. Friedel, P., unpublished.
8. Friedel, P. and Pohlers, A., *QCPE Bulletin*, 1994, **14**, 27–29.
9. Bergmann, J., in RAYFLEX-Seifert X-Ray Diffraction Software, Seifert-FPM GmbH, Freiberg i. Sa. (Germany), 1995.
10. Rietveld, H. M., *Acta Crystallographica*, 1967, **22**, 151–152.
11. Rietveld, H. M., *Journal of Applied Crystallography*, 1969, **2**, 65–71.
12. CERIUS^2 1.5, Molecular Simulations, Cambridge, UK, 1994.
13. Xmol 1.3.1, ftp://ftp.msc.edu/pub/xmol, Minnesota Supercomputer Center, MN, USA, 1995.
14. Williams, T. and Kelley, C., GNUPLOT 3.5, e-mail: info-gnuplot@dartmouth.edu, bug-gnuplot@dartmouth.edu, 1986–1993.
15. Jin, J.-I., Lee, S.-H. and Park, H.-J., *Polymer Bulletin*, 1988, **20**, 19–23.
16. Erdemir, A. B., Johnson, D. J. and Tomka, J. G., *Polymer*, 1986, **27**, 441–447.
17. Jung, B. and Schürmann, B. L., *Molecular Crystals and Liquid Crystals*, 1990, **185**, 141–153.
18. Blackwell, J., Gutierrez, G. A. and Chivers, R. A., *Macromolecules*, 1984, **17**, 1219–1224.
19. Karacan, I., Johnson, D. J. and Tomka, J. G., *Polymer Preprints (American Chemical Society, Division of Polymer Chemistry)*, 1992, **33**, 333–334.
20. Johnson, D. J., Karacan, I. and Tomka, J. G., *Polymer*, 1991, **32**, 2312–2318.
21. Johnson, D. J., Karacan, I. and Tomka, J. G., *Polymer*, 1990, **31**, 8–14.
22. International Tables for Crystallography, Kluwer, Dordrecht, 1992–1993.
23. Van Gunsteren, W. F. and Berendsen, J. C., *Angewandte Chemie*, 1990, **102**, 1020–1055.
24. Weiner, S. J., Kollman, P. A., Nguyen, D. T. and Case, D. A., *Journal of Computational Chemistry*, 1986, **7**, 230–252.
25. Larson, A. C. and von Dreele, R. B., in *General Structure Analysis System*, Los Alamos National Laboratory, NM, USA, 1985–1996.